Chemical oxidation of selenite to selenate: Evaluation of reactive oxygen species and O transfer pathways

Pooya Paydary [a], Alexandra E.P. Schellenger [a], Minerva Teli [b], Deb P. Jaisi [c], Annalisa Onnis-Hayden [a], Philip Larese-Casanova [a,*]

[a] Department of Civil and Environmental Engineering, Northeastern University, Boston, MA, USA
[b] Department of Civil and Environmental Engineering, University of California, Berkeley, Berkeley, CA, USA
[c] Department of Plant and Soil Sciences, University of Delaware, 531 S College Ave., Newark, DE 19716, USA

ARTICLE INFO

ABSTRACT

Naturally occurring selenium is usually found in shales, mostly in the form of reduced selenides or elemental selenium metal. In contrast, downstream oxic waters and soils contain the oxidized forms of selenium as the oxyanions selenite ($HSeO_3^-$, SeO_3^{2-}) and selenate (SeO_4^{2-}). Whereas the oxidation of selenides to selenium oxyanions is possible in the presence of O_2, the actual mechanisms of oxidation, and selenate formation in particular, are not fully understood. In this work, reactive oxygen species were evaluated for selenite oxidation within batch reactors at circumneutral pH. Complete selenite oxidation to selenate by ozone (O_3) and hypochlorite (OCl^-, as a positive control) occurred within minutes and seconds, respectively. Partial oxidation of selenite to selenate by hydrogen peroxide required two weeks reaction at 2 M H_2O_2. Hydroxyl radicals were generated by photo-catalytic decomposition of H_2O_2 and oxidized selenite completely within six hours. Singlet oxygen, superoxide, and peroxynitrite were not observed to oxidize selenite. By using selenite and H_2O with varying $\delta^{18}O$ isotopic compositions in oxidation experiments, it was possible to infer the two different sources of O during selenate formation. Selenate inherits three O from selenite and is suggested to acquire the fourth O via O transfer from the oxidants studied here.

1. Introduction

The presence of selenium oxyanions in surface waters is caused by weathering of selenium-rich minerals, release of selenium-laden industrial wastes, or deposition of selenium-containing particulate emissions (Stillings and Amacher, 2010; Lemly, 2004). In the subsurface in the western United States, selenium is found within Cretaceous marine sedimentary shales (Stillings and Amacher, 2010; Seiler et al., 1999; Martens and Suarez, 1997; Kulp and Pratt, 2004; Presser and Swain, 1990), crude oil associated with these shales (Presser, 1994), and the Phosphoria formation (Stillings and Amacher, 2010), mostly in the form of reduced Se(-II) selenides within substituted pyrite (FeS_2), ferroselite ($FeSe_2$), dzharkenite ($FeSe_2$) and organo-selenium compounds as well as elemental Se^0 metal. In contrast, it is the oxidized forms of sele- nium— the oxyanions selenite (Se(IV), SeO_3^{2-}), hydrogenselenite (Se (IV), $HSeO_3^-$), and selenate (Se(VI), SeO_4^{2-}) which are more thermody-namically favorable under ambient atmospheric conditions—that are found in downstream waters (Martens and Suarez, 1997) and soils

(Presser and Swain, 1990; Luoma and Presser, 2009) and refinery pro-cessing waters from desalting operations (Lawson and Macy, 1995). Dissolved selenium oxyanions can then be transported through surface and subsurface waters, where they can pose health risks to humans and ecosystems at elevated concentrations (Lemly, 2004; Luoma and Presser, 2009). Selenate is generally thought to form from reduced selenium by oxidative dissolution, but the actual chemical processes responsible for selenite, selenium, or selenide oxidation to selenate in natural settings remains undetailed. Despite several laboratory studies exploring these redox changes in selenium by oxidative weathering (Kulp and Pratt, 2004; Howard III, 1977; Masscheleyn et al., 1990; Strawn et al., 2002), the mechanisms and conditions of how selenate acquires its oxygen atoms are not fully understood.

Throughout the literature there are conflicting and incomplete an-ecdotes of whether abiotic selenite oxidation to selenate by O_2 can occur at all, and those reporting selenate formation do so only under alkaline pH with soil present, which could support other oxidants than O_2 (Howard III, 1977; Masscheleyn et al., 1990; Lakin, 1961). Selenide-

bearing iron minerals can be readily oxidized by O_2 to elemental selenium, which can oxidize much more slowly to selenite (Stillings and Amacher, 2010; Howard III, 1977; Masscheleyn et al., 1990; Dowdle and Oremland, 1998; Sarathchandra and Watkinson, 1981). Chemical selenite oxidation by hydrogen peroxide is relatively fast in strongly acidic medium (Hughes and Martin, 1955), but others report little (Liu et al., 2019) to no (Albrecht et al., 1999) oxidation of selenite by H_2O_2 at pH 7 or above. Other oxidants capable of selenite oxidation and evaluated for water treatment applications have included TiO_2 photocatalysis (Gruebel et al., 1995), permanganate (Liu et al., 2019; Dikshitulu and Babu, 2009), hypochlorous acid (Liu et al., 2019; Boegel and Clifford, 1986), hypobromous acid (Liu et al., 2019), monochloramine (Liu et al., 2019), and ozone (O_3) (Liu et al., 2019). Manganese oxides, which are found in subsurface environments, have been reported to slowly oxidize selenite to selenate after surface adsorption and a reduction of Mn(IV) to Mn(II) (Scott and Morgan, 1996). A small amount of biotic selenite oxidation has been reported by a sulfite-oxidizing bacteria (Dowdle and Oremland, 1998) and a soil bacterium (Sarathchandra and Watkinson, 1981) and has been speculated to occur fortuitously by non-specific sulfite-oxidizing enzymes. More recently, an abiotic pathway for elemental selenium oxidative dissolution was reported and involves microbially-produced extracellular reactive sulfur species (sulfide, sulfite, and thiosulfate) solubilizing selenium in Se-S oxyanions (Goff et al., 2019).

Nevertheless, there are other dissolved, natural oxidants that need evaluation for which selenite oxidation, including photogenerated reactive oxygen species (ROS). The primary objective of this work is to test if dissolved ROS relevant to surface waters can oxidize selenite to selenate. Photochemically-driven reduction of O_2 occurs naturally in surface waters, and sequential electron transfer produces highly reactive intermediates superoxide (O_2^-), hydrogen peroxide (H_2O_2), and hydroxyl radicals ($^\bullet OH$). O_2 reduction and ROS generation by light can be facilitated by dissolved organic matter which gets photochemically reduced and can reduce O_2 to O_2^-, H_2O_2, and $^\bullet OH$ (Garg et al., 2011; Vaughan and Blough, 1998). Organic matter can also absorb light and in an excited state react with ground state triplet oxygen to create singlet oxygen ($^1O_2$) (Zepp et al., 1977; Cory et al., 2009). Other routes of hydroxyl radical formation include photochemical cleavage of $^\bullet OH$ from H_2O_2 (Zellner et al., 1990), NO_3^- (Zellner et al., 1990; Jankowski et al., 1999; Zafiriou and True, 1979), and NO_2^- (Zellner et al., 1990; Jankowski et al., 1999). The possible role of hydroxyl radicals in TiO_2 photocatalysis of selenite to selenate (Gruebel et al., 1995) strongly suggests hydroxyl radicals formed by other photogeneration pathways could also serve as a natural selenite oxidant similar to oxidation of As(III) to As(V) (Kim et al., 2014). Lastly, O_3, already shown to be a facile oxidant of selenite in the drinking water treatment context (Liu et al., 2019), also has relevance to contaminant oxidation in natural systems. O_3 can be formed when NO_x and volatile organic compounds react with sunlight (Ripperton et al., 1971) or by stratospheric intrusion to cumulonimbus clouds (Winterrath et al., 1999). O_3 could potentially encounter reduced selenium when soils, waters, or mineral formations are exposed to the atmosphere. O_3 diffusion to soils has been reported to alter microbial community structure and function (Zhang et al., 2019). Ground-level ozone concentrations near industrial activity can exceed 100 ppb$_v$ (Sillman, 1999), and elevated ozone concentrations have been observed in rural forests (Li et al., 2018) and rural petroleum processing areas (Vijayaraghavan et al., 2016). Ozone has been studied as a potential oxidant of organoselenium in the context of atmospheric environments (Rael et al., 1996), and ozone encounters with inorganic selenium in clouds might be possible.

The secondary objective of this work is to understand the O transfer mechanism of selenate formation, that is, after inheriting three O from selenite, whether selenate acquires its fourth O from the oxidant by way of direct O transfer or from ambient water. There is some evidence that H_2SeO_3 oxidation to H_2SeO_4 involves a transfer of O from the oxidant H_2O_2 accompanying electron transfer for selenic acid formation (Lunenok-Burmakina et al., 1967). In a similar manner, enzymatic oxidation

of nitrite to nitrate involves incorporation of one O from the oxidant O_2 (DiSpirito and Hooper, 1986). In addition to providing useful insight to the selenite oxidation mechanism, identifying the source of the fourth O in SeO_4^{2-} has value in O stable isotope systematics in selenium redox cycling. Specifically, because selenate-$\delta^{18}O$ values are stable at environmental temperatures and pH (Okumura and Okazaki, 1973a; Hall and Alexander, 1940; Kaneko and Poulson, 2012), $\delta^{18}O_{SeO4}$ values could be used to trace dissolved selenate origin and transport in water. Different selenite oxidation processes might imprint different $\delta^{18}O$ values on selenate. Selenate inherits three O from selenite, and because selenite O rapidly exchanges all its O with ambient H_2O (Okumura and Okazaki, 1973b), at least three O in selenate will be reflected by $\delta^{18}O_{H2O}$ values. Or, if H_2O is the source of the fourth O in selenate, $\delta^{18}O_{SeO4}$ might be dictated entirely by $\delta^{18}O$ of H_2O (plus some fractionation caused by O transfer), which is based on latitude-dependent precipitation.

Accordingly, batch reactor experiments were conducted to evaluate different reactive oxygen species for their ability to oxidize selenite to selenate. The O transfer mechanisms participating in selenate formation are inferred by ^{18}O tracing. The results are interpreted to identify which ROS might be important in the redox cycling of selenium in nature and to highlight influences on $\delta^{18}O$ values of selenate.

2. Materials and methods

2.1. Experiments

Deionized water (>18 MΩ) and chemicals purchased at high purity were used in all experiments. A summary of conditions for all batch reactor experiments appears in Table S1 in the Appendix. Millimolar concentrations of selenite were required for sample mass requirements for isotopic measurements. Kinetic experiments that evaluated the rate of selenite oxidation to selenate by chemical and photochemical oxidants described below were carried out using a solution of ~1 mM selenite buffered at pH 7.0 with 5 mM phosphate buffer in deionized water unless otherwise noted. At this pH, selenite (pKa$_2$ 8.3) is present as 95% $HSeO_3^-$ and 5% SeO_3^{2-}, but are collectively referred to as selenite for simplicity. Aqueous samples were taken over time and were either analyzed for selenite and selenate concentrations immediately or stored at 4 °C after cessation of the reaction by removing the samples from light or quenching the reaction, such as by addition of 1 mM sulfite to samples with dissolved ozone present.

Batch reactors with hydroxyl radicals as the primary oxidant were performed via photochemical conversion of H_2O_2. Solutions of selenite with 200 mM H_2O_2 were irradiated at 950 W with a Xe arc lamp (ozone-free) (Oriel Instruments) and a 90° reflecting mirror for 8 h under magnetic stirring. The distance between lamp and solution was 20 cm. To prevent temperature rise as a result of light radiation, the experiment was performed in a water jacketed reactor. Solution temperature was monitored during the experiment and was kept at 20 $\pm$ 1 °C. Dissolved nitrate (200 mM) and nitrite (200 mM) were also separately tested instead of H_2O_2 for photochemical generation of hydroxyl radicals. Crystal violet was also tested as a positive control. Batch reactors with H_2O_2 alone as the oxidant were conducted with selenite and 2 M H_2O_2 and stored in the dark under static conditions.

The photochemical experiment that tested singlet oxygen as an oxidant involved irradiating, under magnetic stirring, solutions of selenite with rose Bengal (0.25 mM) as a photosensitizer. Rose Bengal is expected to absorb light within ~500–600 nm to form an excited state that transfers energy to ground-level (triplet) state $^3O_2$ to form $^1O_2$. Furfuryl alcohol was irradiated as a positive control.

Ozonation experiments were performed by bubbling ozone gas using an ozone-insensitive stone diffuser through a solution of 0.1 mM tert-butanol (as a hydroxyl radical scavenger) and selenite in a 50 ml glass bottle for 20 min under magnetic stirring. In one experiment, equimolar concentrations (10 mM) of selenite and sulfite were present to compare

competitive ozonation rates. Ozone was produced using a Triogen ozone generator fed with 99.999% O_2 (Airgas). All ozone batch reactors were performed in one setting after time for maximum ozone generation was reached, in order to utilize the same ozone flow rate across all kinetic experiments or all isotope tracing experiments.

The batch reactor with sodium hypochlorite as the oxidant was conducted with 10 mM NaOCl in 1 mM selenite buffered at pH 7.0 with 5 mM MOPS buffer. Concentration timecourses were not measured in our solutions of chlorine and selenite because selenite concentrations decreased below detection limit before time to measurement.

Peroxynitrite and potassium superoxide were also separately tested as a possible oxidant by addition of powder (10 mM) to a 1 mM selenite solution buffered at pH 7.0 with 5 mM phosphate. These experiments were performed at 4 °C due to the compound's instability at room temperature.

The experiments that measured $\delta^{18}O_{SeO4}$ values after reaction with selected oxidants were conducted at higher initial selenite concentrations (5 mM) without buffer to prevent interferences from phosphate on $\delta^{18}O_{SeO4}$ analysis or to prevent organic buffer parallel reactions, if any, with ROS. The selenite solutions were prepared in deionized water with varying $\delta^{18}O$ values (−4, 5, 10, 20, 30, and 35‰) which were made by addition of 97 atom% enriched ^{18}O H_2O (Cambridge Isotope Laboratories, Inc.). The pH of these solutions was adjusted to 7.0, and selenite was allowed to equilibrate with H_2O at least overnight. Aqueous samples for initial $\delta^{18}O_{H2O}$ were taken prior to the addition of oxidants, and aqueous samples for $\delta^{18}O_{H2O}$ and $\delta^{18}O_{SeO4}$ were taken at the end of the reaction timecourse. Samples for $\delta^{18}O_{H2O}$ were stored in 2-ml crimp-sealed glass vials, and samples for $\delta^{18}O_{SeO4}$ were processed immediately without storage (Section 2.2). The solution pH was monitored during reaction and maintained close to 7.0 using HCl and NaOH titrants. Temporary pH deviation, if any, was less than 0.7 pH units.

2.2. Analytical methods

Dissolved selenite, selenate, sulfite, and sulfate concentrations were quantified by anion chromatography with a Dionex DX-120 instrument operating with a IonPac AS9-HC analytical column and a 11 mM Na_2CO_3 eluent at 1.0 ml min^{-1} flow rate (Schellenger et al., 2021). Dissolved ozone concentrations were measured colorimetrically by method 4500-O_3 B (Rice et al., 2012). Benzoic acid, its oxidation products (4-hydroxybenzoic acid, 3-hydroxybenzoic acid, and 2,5-dihydroxybenzoic acid), and furfuryl alcohol were measured by high pressure liquid chromatography (HPLC, Agilent 1260 Infinity Quaternary LC) with a C18 column, a 1.0 ml min^{-1} flow rate, an eluent of 20% methanol with 80% 25 mM phosphate buffer at pH 2.1, and UV detection, from a modified version of a previous method (Sánchez-Polo et al., 2005). Crystal violet concentrations were measured spectrophotometrically at 590 nm by comparison to standard solutions of known concentration (Corsaro, 1964).

$\delta^{18}O$ values of water were measured with a DELTAplusXP isotope ratio mass spectrometer coupled to a Thermo-Finnigan Gasbench II preparation and introduction system (Yale Analytical and Stable Isotopic Center, YASIC) (Larese-Casanova and Blake, 2013). Water samples were injected to a 12 ml exetainer previously flushed with Helium and 0.3% CO_2 gases and allowed to equilibrate at 25 °C for at least 24 h. Headspace samples were introduced to mass spectrometer and detected for the isotopic ratio of $^{18}O/^{16}O$. The $\delta^{18}O$ values were calibrated to the Vienna Standard Mean Ocean Water (VSMOW) scale using in-house standard waters. Instrument accuracy to VSMOW scale was further checked with periodic measurements of VSMOW2 (0‰) and SLAP2 (−55.5‰) waters. Six replicates of each water sample were measured and averaged, and the average of the standard deviations on H_2O $\delta^{18}O$ values was 0.1‰.

$\delta^{18}O$ measurements of selenite and selenate were performed after processing aqueous samples according to a barium selenite or barium selenate precipitation method (Larese-Casanova and Blake, 2013) which

requires >1 mM of Se. For solutions containing both selenite and selenate (i.e. after incomplete selenite oxidation), the dissolved selenite was first removed by a $Ce_2(SeO_3)_{3(s)}$ precipitation method (Xia et al., 2020). The $BaSeO_{3(s)}$ or $BaSeO_{4(s)}$ was collected, dried, and weighed to determine selenium recovery (typically 95–100%). $\delta^{18}O$ values were measured using a Thermo thermochemolysis elemental analyzer (TC/EA) (reactor temperature 1450 °C and GC column temperature 95 °C) and a Thermo Delta V mass spectrometer coupled via a Confolo IV interface (Environmental Isotope System Lab, University of Delaware). Approximately 300 mg of each $BaSeO_{3(s)}$ or $BaSeO_{4(s)}$ sample was placed in Costech pressed silver capsules and measured. Samples were calibrated to the VSMOW scale using an in-house barium selenate standard of −10.3‰, an in-house silver phosphate standard of 10‰, and IAEA-601 benzoic acid with value + 23.3‰. Across all time points, samples were measured in triplicate and averaged, and the averaging of the standard deviations on $BaSeO_{3(s)}$ or $BaSeO_{4(s)}$ $\delta^{18}O$ values was 0.4‰.

3. Results and discussion

3.1. Evaluation of photogenerated reactive oxygen species

The reaction kinetics specific to our required experimental conditions were first characterized to confirm the time to complete selenite oxidation and to compare briefly the relative rates of selenite oxidation by several different ROS. First, photogenerated •OH readily oxidized
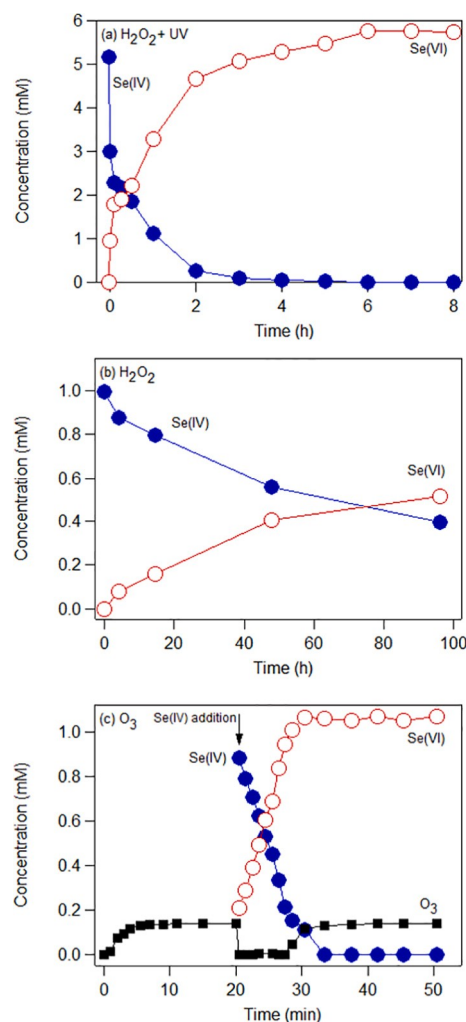

Fig. 1. Reaction timecourses for selenite oxidation to selenate at pH ~7 with (a) 200 mM H_2O_2 + UV light, (b) 2 M H_2O_2 alone, and (c) ozone.

selenite to selenate at pH 7.0. When 200 mM H_2O_2 was illuminated with UV light, ~5 mM selenite was oxidized within 3 h to ~5 mM selenate (Fig. 1a). Neither direct photolysis alone nor 200 mM H_2O_2 alone within control reactors were able to oxidize any selenite (Fig. S1 in the Appendix), leaving the photogenerated $^\bullet OH$ as the likely oxidant, which forms according to $H_2O_2 + hv \rightarrow 2^\bullet OH$. To further confirm the presence of $^\bullet OH$ created within our setup, a solution of 1 mM benzoic acid was also illuminated at pH 7.0 and with either 200 mM H_2O_2 or 200 mM NO_3^-, and the oxidation products 4-hydroxybenzoic acid, 3-hydroxybenzoic acid, and 2,5-dihydroxybenzoic acid were detected by HPLC, which are typically formed by $^\bullet OH$ addition to the benzene ring (Klein et al., 1975).

The rate of selenite oxidation depended on the source of $^\bullet OH$. When dissolved nitrite was illuminated, only 0.1 mM selenite was oxidized within 3.5 h, and no observable selenite oxidation occurred when dissolved nitrate was present (Fig. S1). The faster rate with H_2O_2 compared to nitrate and nitrite at the same concentrations could be due to two $^\bullet OH$ forming from H_2O_2 instead of one and a possibly more facile or faster -OH bond cleavage. The much higher selenite reactivity with H_2O_2 is consistent with H_2O_2 having the greater $^\bullet OH$ quantum yield (0.98, compared to 0.07 for NO_2^- and 0.02 for NO_3^-), as measured by photolysis at 308 nm and 298 K (Zellner et al., 1990). The greater reaction rate of H_2O_2 compared to NO_3^- and NO_2^- was also confirmed in our setup using the organic probe compound crystal violet (Fig. S2). $^\bullet OH$ were also implicated as the oxidant (in addition to photogenerated holes) in selenite oxidation during illumination of a semiconducting TiO_2 photocatalyst (Gruebel et al., 1995). Our results support the notion that dissolved $^\bullet OH$ alone formed from O bond cleavage from homogenous solutes can also oxidize selenite fairly rapidly.

While 200 mM H_2O_2 alone was not reactive to selenite, H_2O_2 alone at 10-fold higher concentrations (2 M) at pH 7.0 was able to oxidize only 0.6 mM selenite to selenate over four days (Fig. 1b). This observation is consistent with no observed selenite oxidation at circumneutral pH and low H_2O_2 concentrations (Albrecht et al., 1999). The rate of oxidation by H_2O_2 can be enhanced at low pH where selenious acid is the dominant selenium species (Hughes and Martin, 1955).

Selenite transformation and selenate formation by $^\bullet OH$ and by H_2O_2 alone could be modeled with a pseudo-first-order rate model with the concentration profile equations $C = C_o e^{-kSeIVt}$ for selenite loss and $C = C_o(1-e^{-kSeVIt})$ for selenate formation. Fig. S1 summarizes the fitted data for all experimental replicates for several oxidants, and fitted coefficients appear in Table 1. The rate coefficients k_{SeIV} and k_{SeVI} apply to these conditions where $^\bullet OH$ or H_2O_2 are at unlimited supply compared to selenite and for circumneutral pH. The rate coefficients for selenite loss k_{SeIV} were similar and within a factor of 2 for the rate coefficients of selenate formation k_{SeVI}. Selenite oxidation with $^\bullet OH$ from H_2O_2 illumination was repeated in triplicate, and similar rate coefficients were

observed, indicating good reproducibility. The rate coefficients for $H_2O_2 + UV$ were approximately 100-fold greater than the coefficients for $NO_3^- + UV$ or for H_2O_2 alone.

A second-order rate expression between H_2O_2 and selenite was recently reported, based on observations of H_2O_2 loss under constant selenite concentrations (Liu et al., 2019). Their kinetic analysis gave a second order rate coefficient $2.3 \times 10^{-5}\,M^{-1}s^{-1}$ at pH 7.0, which for our conditions (2 M H_2O_2, pH 7.0) would produce a predicted pseudo-first-order k_{SeIV} of 0.2 h^{-1}, a value that is about 20 times higher than our measured value of 0.011 h^{-1}.

Singlet oxygen was also explored for selenite oxidation, but no selenate formation occurred (Fig. S1). $^1O_2$ was generated photochemically by illuminating a photosensitizer, rose Bengal, with O_2-saturated water. The presence of $^1O_2$ was first confirmed using the organic probe compound furfuryl alcohol (Fig. S3) which is known to become oxidized to furfural by $^1O_2$ (Haag et al., 1984). However, no selenite oxidation was observed with rose Bengal illumination over 5 h. The superoxide anion O_2^- was tested by addition of potassium superoxide powder to selenite solution in a single trial, and no selenite oxidation was observed. Although not photochemically generated, peroxynitrite (HOONO) has been hypothesized to oxidize selenite to selenate under circumneutral pH (Albrecht et al., 1999), but our experiment exposing selenite to peroxynitrite also produced no selenite oxidation. Selenite does not appear to be susceptible to oxidation by these ROS.

The observed kinetic rates indicate that among all possible photogenerated oxidants in natural waters, $^\bullet OH$ are the fastest oxidants for selenite. In addition, H_2O_2, as opposed to NO_3^- and NO_2^-, might be the most likely photosensitizer for $^\bullet OH$ formation in selenite oxidation. H_2O_2 can form in surface waters by sunlight illumination, and concentrations up to several μM are possible (Cooper et al., 1988). $^\bullet OH$ formation from nitrate or nitrite might also be important if concentrations are significantly higher than H_2O_2. Nitrate concentrations up to 1 mM are possible in agriculture-impacted waters but more commonly in the 1–100 μM range (US EPA, 1987). While our results show H_2O_2 is more photosensitive compared to nitrate at equimolar concentrations, nitrate can be responsible for up to ~90% of $^\bullet OH$ production in surface waters (Hoigné et al., 1988; Mostofa et al., 2013)
.

3.2. Selenite oxidation by ozone

The kinetics of selenite oxidation by O_3 was recently reported, based on measurements of O_3 loss under excess selenite concentrations (Liu et al., 2019). Here, O_3 needed to be continuously bubbled into selenite solution because the selenite concentration (1–5 mM) was above the dissolved ozone saturation concentrations (about 150 uM at room temperature under our synthesis conditions). After O_3 saturation was achieved in 20 min, selenite solution was added, and some initial selenite oxidation to selenate occurred instantaneously due to the present dissolved O_3 which was immediately consumed (Fig. 1c). The selenite removal and selenate formation was subsequently linear during further ozone dissolution. The linear kinetic profile is a strong indication of mass transfer limitations caused by ozone transfer via thin film diffusion into water, and such behavior can be modeled with the zero-order reaction rate law $C = C_o - k^0_{SeIV}t$ for selenite loss and $C = C_o + k^0_{SeVI}t$ for selenate formation. Duplicate experiments produced similar values of k^0_{SeIV} and k^0_{SeVI} (Table 1) for the range of linear concentrations (Fig. S1). O_3 decomposition to $^\bullet OH$, and therefore a creation of a second oxidant, is not expected at pH 7.0 (Sotelo et al., 1987).

These measured reaction coefficient values are specific to our gaseous O_3 settings. To better estimate a reaction rate more intrinsic to selenite and more relevant to environmental conditions, a second experiment was performed adding O_3 to a solution containing both selenite and sulfite at equimolar concentrations in order to compare their relative rates. Selenite and sulfite concentrations decreased linearly over 10 min, and selenate and sulfate concentrations concomitantly

Table 1
Reaction rate coefficients for selenite oxidation and selenate formation by $^\bullet OH$, H_2O_2, and O_3 oxidants at pH 7.0. Model fits appear in Fig. 1 and Fig. S1. Rate coefficients are modeled values ± one standard deviation on the model fit. Experiments with $H_2O_2 + UV$ were performed in triplicate, and experiments with O_3 were performed in duplicate.

Oxidant	Se(IV) rate coefficient	R^2	Se(VI) rate coefficient	R^2
First-order reactions	$k^I_{Se(IV)}$ (hr^{-1})		$k^I_{Se(VI)}$ (hr^{-1})	
$H_2O_2 + UV$ 1	2.61 ± 0.72	0.98	1.05 ± 0.20	0.91
$H_2O_2 + UV$ 2	1.35 ± 0.31	0.96	0.80 ± 0.07	0.91
$H_2O_2 + UV$ 3	2.76 ± 0.46	0.95	1.56 ± 0.12	0.85
H_2O_2	0.011 ± 0.001	0.98	0.009 ± 0.001	0.96
$NO_3^- + UV$	0.027 ± 0.01	0.80	1.79 ± 0.77	0.53
Zero-order reactions	$k^0_{Se(IV)}$ (hr^{-1})		$k^0_{Se(VI)}$ (hr^{-1})	
O_3 1	0.09 ± 0.01	0.99	0.10 ± 0.01	0.99
O_3 2	0.14 ± 0.01	0.99	0.15 ± 0.01	0.99

increased linearly (Fig. S1). Sulfite was oxidized preferable compared to selenite, with the zero-order rate coefficient for sulfite oxidation (46.2 h^{-1}) being approximately 20-fold greater than that for selenite oxidation (2.4 h^{-1}). Selenite oxidation by O_3 in nature could thus be envisioned as 20-fold slower than sulfite oxidation. The second-order rate coefficients for ozone oxidation of bisulfite ($8.0 \times 10^5 M^{-1} s^{-1}$) and sulfite ($1.3 \times 10^9 M^{-1} s^{-1}$) have previously been recorded under acidic conditions (Liu et al., 2001). The 20-fold lower slope for selenite compared to sulfite species for oxidation by ozone here at pH 7.0 under mass transfer limiting conditions may suggest that biselenite and selenite could have second-order rate coefficients on the order of $10^4 M^{-1} s^{-1}$ and $10^8 M^{-1} s^{-1}$, respectively, although such values might be applicable only at acidic pH. A recent report (Liu et al., 2019) provides a second-order rate coefficient for selenite ozonation applicable to circumneutral pH as 513 $M^{-1} s^{-1}$, determined under excess selenite conditions at pH 7.0 but not with continuous O_3 gas bubbling and therefore without any mass transfer limitation.

3.3. Selenate formation pathways

Because selenate will inherit three O from selenite, the control on selenite $\delta^{18}O$ values was first addressed. The complete mixing of selenite O with ambient H_2O has been reported previously (Okumura and Okazaki, 1973b), but these observations were noted at elevated temperatures and extreme pH values (1 and 14). Complete O mixing between selenite and H_2O under our experimental conditions and prepared $\delta^{18}O$ waters was first confirmed (Fig. 2). The slope of the correlation between $\delta^{18}O$ of selenite and $\delta^{18}O$ of H_2O is nearly 1, which shows 100% of O in selenite (all three O atoms) is dictated by the $\delta^{18}O$ value of solvent water. The intercept of the relationship (3.6) represents the fractionation value $F_{SeO3-H2O}$ of 3.6‰ for this exchange step at room temperature.

It can thus be concluded that initial selenite prior to oxidation holds a $\delta^{18}O$ value entirely determined by the solvent water at the ambient temperature. Consequently, after oxidation to selenate, those three of the four O atoms in selenate are inherited from selenite and must reflect $\delta^{18}O$ of solvent water. The fourth O atom in selenate must be acquired either from the oxidant or the solvent water as well. The $\delta^{18}O$ value of selenate can then be described as

$$\delta^{18}O_{SeO4} = \tfrac{3}{4} \delta^{18}O_{SeO3} + \tfrac{1}{4} \delta^{18}O_? + F_{SeO4-SeO3} \qquad (1)$$

where $\delta^{18}O_{SeO3}$ is the $\delta^{18}O$ value of selenite, $\delta^{18}O_?$ represents the $\delta^{18}O$ value of the unknown source, and $F_{SeO4-SeO3}$ is the O fractionation for the oxidation step. Substituting the selenite-water O exchange equation yields.

$$\delta^{18}O_{SeO4} = \tfrac{3}{4} \left(\delta^{18}O_{H2O} + F_{SeO3-H2O} \right) + \tfrac{1}{4} \delta^{18}O_? + F_{SeO4-SeO3} \qquad (2)$$

If the fourth O comes from H_2O, $\delta^{18}O_?$ becomes $\delta^{18}O_{H2O}$, and Eq. (2) becomes.

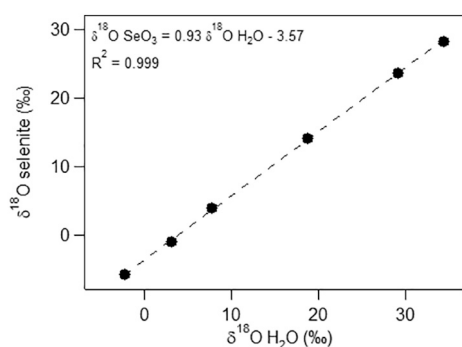**Fig. 2.** Linear correlation between $\delta^{18}O_{SeO3}$ and $\delta^{18}O_{H2O}$ after 24 h equilibration at room temperature.

$$\delta^{18}O_{SeO4} = \delta^{18}O_{H2O} + \tfrac{3}{4} F_{SeO3\_H2O} + F_{SeO4\_SeO3} \qquad (3)$$

In this case, $\delta^{18}O_{SeO4}$ is linearly dependent on $\delta^{18}O_{H2O}$, and Eq. (3) can be expressed as a linear equation of $\delta^{18}O_{SeO4}$ versus $\delta^{18}O_{H2O}$ with a slope of 1. If the fourth O is donated by the oxidant, $\delta^{18}O_?$ becomes $\delta^{18}O_{ox}$, and Eq. (2) becomes.

$$\delta^{18}O_{SeO4} = \tfrac{3}{4} \delta^{18}O_{H2O} + \tfrac{1}{4}\delta^{18}O_{ox} + \tfrac{3}{4} F_{SeO3-H2O} + F_{SeO4-SeO3} \qquad (4)$$

In this case, Eq. (4) plotted as $\delta^{18}O_{SeO4}$ versus $\delta^{18}O_{H2O}$ would have a slope of 0.75. Therefore, the two reaction pathways could be distinguished by the slope value of either Eqs. (3) or (4). The intercept of such regression line would be a combination of the isotopic composition of the oxidant, the temperature-dependent equilibrium O fractionation between selenite and water, and the O fractionation for the oxidation step which would also be oxidant-specific. To determine the origin of the fourth O in selenate, selenite was oxidized in waters of varying $\delta^{18}O_{H2O}$ values, and the subsequent $\delta^{18}O_{SeO4}$ were measured and plotted against $\delta^{18}O_{H2O}$ values for slope calculation (1 or 0.75). Based on the evaluation of reaction rates with ROS above, the oxidants chosen for pathway analysis were H_2O_2 UV, H_2O_2 alone, O_3, and HOCl as a positive control.

Photochemically-produced hydroxyl radicals were induced from H_2O_2 in each of the six waters with added selenite, and the reaction was allowed to proceed until complete selenate formation. The slope of 0.73 in Fig. 3a suggests the fourth O does not come from water and strongly implies the fourth O comes from $^\bullet$OH itself. With an increase in selenium oxidation state from selenite to selenate and each O in $^\bullet$OH capable of accepting one electron, the presumed reaction stoichiometry at pH 7.0 is $HSeO_3^- + 2^\bullet OH \rightarrow SeO_4^{2-} + H_2O$ to satisfy the two electron, one O transfer process. The O from one $^\bullet$OH is proposed to form a double bond with selenium at the selenium lone pair of electrons to form the tetrahedral SeO_4^{2-} (Fig. 4, reaction 1).

Selenite oxidation by H_2O_2 alone in varying $\delta^{18}O$ waters also resulted in a slope of nearly 0.75 in Fig. 3b and implies one O transfers directly from H_2O_2. A direct O transfer from H_2O_2 to biselenite and the resulting intermediate is proposed (Fig. 4, reaction 2). However, the reaction of O transfer from H_2O_2 was first proposed between selenious acid and H_2O_2 at acidic conditions and could involve two different reaction intermediates (Hughes and Martin, 1955). The formation of peroxyselenite (HOOSeOOH) was proposed to first occur by combining H_2O_2 and SeO_2 (Fig. 4, reaction 3). SeO_2 is the dehydrated form of H_2SeO_3 but may be present only at acidic conditions and in low concentrations. Peroxyselenite was proposed to react with either biselenite in a one O transfer process (Fig. 4, reaction 4) or with SeO_2 in a two O transfer process (reaction 5). The former would result in one O from H_2O_2 incorporated into selenate and produce a slope of 0.75, but in the latter selenate would inherit two O from H_2O_2 and result in a slope of 0.5, an option which must be eliminated as a possibility. Only reactions 2 and 4 are consistent with the relationship in Fig. 4, and with SeO_2 rare at pH 7.0, the direct O transfer reaction might be most likely.

Ozonation of selenite also resulted in a slope of 0.73 in Fig. 3c suggestive of one O transfer from O_3 via a reaction intermediate described in reaction 6. O_3 is assumed to have its single O-O bond (the one easiest to break) oriented to biselenite's lone pair of electrons, and the resonance structure shown was presumed based on a favorable electrostatic attraction. A direct O transfer from O_3 to sulfite was also proposed to form a similarly structured intermediate which was supported by ab initio calculations (Liu et al., 2001). Reaction kinetics reported for selenite ozonation were also described as consistent with this O transfer process (Liu et al., 2019).

HOCl was also chosen as another homogeneous, one O oxidant not produced from a separate compound like $^\bullet$OH from H_2O_2. As with the other oxidants studied here, the relationship between $\delta^{18}O_{SeO4}$ and $\delta^{18}O_{H2O}$ has a slope (0.78) close to the theoretical value (0.75) for one O transfer, and so a direct O transfer process from HOCl is envisioned
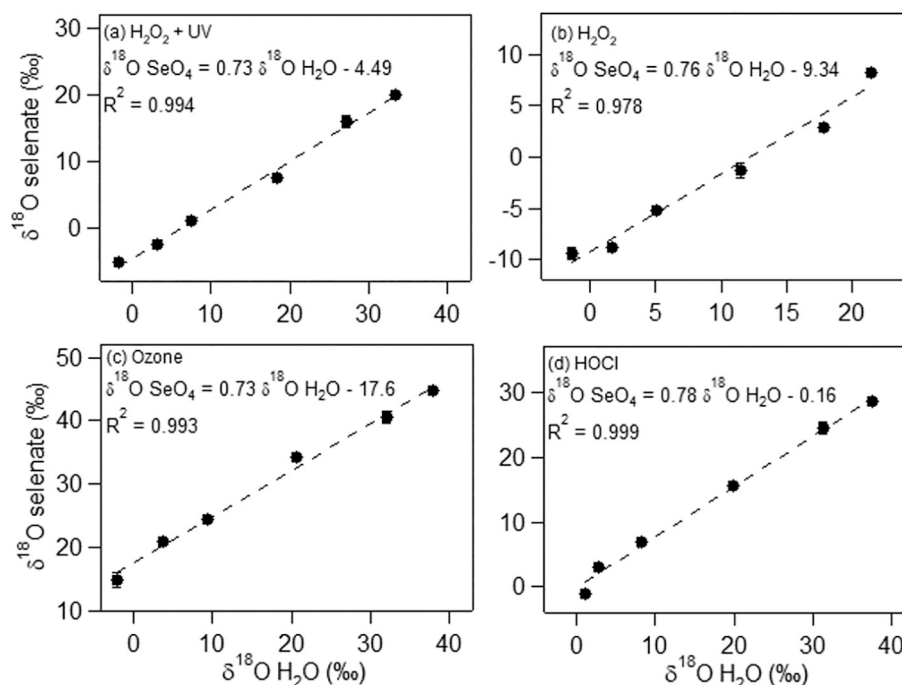
Fig. 3. Linear correlation between $\delta^{18}O_{SeO4}$ and $\delta^{18}O_{H2O}$ after selenite oxidation at pH ~7 by (a) 200 mM H_2O_2 + UV light, (b) 2 M H_2O_2 alone, (c) ozone, and (d) 10 mM HOCl. Error bars are indicated but are typically smaller than the markers.

(reaction 7). However, this is in contrast to a hypothesized mechanism of Cl^+ transfer to form $ClSeO_3^-$ (Liu et al., 2019), which was based on the proposed Cl^+ transfer from HOCl to sulfite to form $ClSO_3^-$ (Fogelman et al., 1989). $ClSO_3^-$ was then suggested to react with two OH^- to form SO_4^{2-}, Cl^-, and H_2O. If such a reaction occurred in our conditions, all four O of selenate would arise from H_2O, bearing a slope of 1.0 in Fig. 3d which was not observed. In the same study, SO_3^{2-} was also proposed to react directly with O in the deprotonated OCl^- due to Cl^- being a favorable leaving group. The isotopic relationship in Fig. 3d suggests this pathway may be the only one occurring for selenite and because our solution at pH 7.0 is 77% HOCl and 23% OCl^-, it is possible both HOCl and OCl^- react with selenite via O transfer.

3.4. Environmental implications

Due to the O transferring from the oxidant during selenite oxidation, the resulting selenate $\delta^{18}O$ values appear to be specific to the oxidation pathway. The intercepts of the linear regressions in Fig. 3 are all different for each of the four oxidants, with a range of 0.16 to 17.6. The intercept, here termed an overall O fractionation between selenate and $H2O$ ($F_{overall}$), represents the sum of the ¼ $\delta^{18}O_{ox}$, ¾ $F_{SeO3-H2O}$, and $F_{SeO4-SeO3}$ values in Eq. (4). $F_{overall}$ should be unique for the oxidant which provides a specific $\delta^{18}O_{ox}$ and $F_{SeO4-SeO3}$ values, and $F_{overall}$ should also be dependent on temperature which influences $F_{SeO3-H2O}$, and $F_{SeO4-SeO3}$. The $F_{SeO3-H2O}$ value at 20 °C is about 3.6, based on the intercept in Fig. 2. However, $\delta^{18}O_{ox}$, $F_{SeO3-H2O}$, and $F_{SeO4-SeO3}$ still need to be determined for the environmentally relevant oxidants at environmentally relevant temperatures in order to calculate an expected $F_{overall}$ specific to an oxidant. Unfortunately, analytical means to measure $\delta^{18}O_{ox}$ for some oxidants such as $^{\bullet}OH$ may not yet exist. Should these values be obtained, a catalog of expected $F_{overall}$ values for all oxidants could be created, and these could be compared to a measured $F_{overall}$ (based on measured $\delta^{18}O_{H2O}$ and $\delta^{18}O_{SeO4}$ from natural waters) to identify the most likely oxidant for selenite in natural settings. The analytical challenges to harvesting enough selenate and measuring $\delta^{18}O_{SeO4}$ from natural waters (Xia et al., 2020) also need to be overcome.

Selenate inheriting three O from H_2O (through selenite mixing O

with H_2O) also implies that $\delta^{18}O_{SeO4}$ in nature will be influenced by the location and hydrologic characteristics of its host water. $\delta^{18}O_{H2O}$ values of surface waters are influenced by $\delta^{18}O_{H2O}$ values in precipitation, which are determined by latitude, temperature, water vapor source, and condensation elevation (Jouzel et al., 2013; Crawford et al., 2013). Evaporation may also enrich $\delta^{18}O_{H2O}$, particularly for closed lakes (Gat, 2010). Across the western United States for example, variations in $\delta^{18}O_{H2O}$ can be up to 18‰ (Henderson and Shuman, 2009). $\delta^{18}O_{SeO4}$ values might therefore be specific to individual lake sources when comparing lakes over large distances or different climates. River systems spanning broad latitude ranges, though, might produce $\delta^{18}O_{SeO4}$ values as a result of mixing multiple selenate sources.

While this study examines four O-bearing oxidants, it is possible that selenite oxidation by a non-O bearing oxidant might also exist in nature. For example, microbial selenite oxidation might not involve an O-bearing oxidant but instead an enzyme-mediated electron transfer and an O incorporation from H_2O. Little is known on the bacterial species and the metabolic pathways responsible for selenite oxidation so far, however. Selenite oxidation has been observed for energy derivation by some sulfite-oxidizing bacteria (Dowdle and Oremland, 1998) and a soil bacterium (Sarathchandra and Watkinson, 1981) and has been speculated to occur fortuitously by non-specific sulfite-oxidizing enzymes. No obligate selenite-oxidizing bacterium has yet been isolated. This class of sulfite-oxidizing enzymes, in particular the well-studied sulfite-dehydrogenase, contains a Mo(VI) or Fe(III) centered group that couples O from H_2O to sulfite while accepting two electrons from sulfite to form sulfate (Bailey et al., 2008). It is expected that such enzymes as well as other monooxygenases capable of selenium oxidation (Andrade et al., 2011) might also incorporate O from H_2O into selenate. If such a process were to control $\delta^{18}O_{SeO4}$ values in nature, the relationship between $\delta^{18}O_{SeO4}$ and $\delta^{18}O_{H2O}$ would be better described by a four O inheritance from H_2O as in Eq. (3).

Additionally, chemical dissolution of elemental selenium by microbially-produced sulfur metabolites could be a significant process in reducing environments (Goff et al., 2019). While this process did not result in selenate formation, subsequent oxidation processes of the formed S-Se compounds now require evaluation as potential routes for
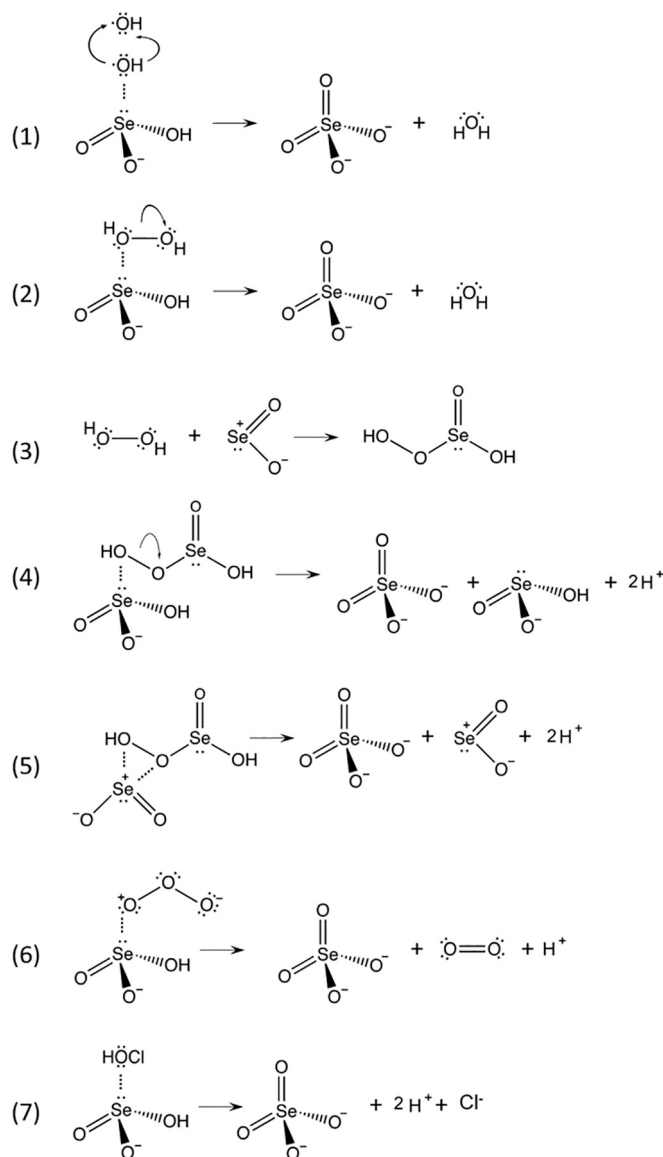
Fig. 4. Proposed selenite oxidation pathways to selenate.

selenate formation. Chemical dissolution of elemental selenium is also possible by hydroxyl radicals (Gao et al., 2002) and hydrogen peroxide (Lu et al., 2017), and these reports suggest or confirm selenium oxyanion formation. Selenate could possibly be formed directly from Se(0) oxidation, and how these processes affect $\delta^{18}O$ of selenate requires evaluation. If dissolved selenite forms as an intermediate but oxidizes before O exchange with water, $\delta^{18}O_{SeO4}$ might not be influenced by $\delta^{18}O_{H2O}$ and only by the oxidant $\delta^{18}O$.

The results of this work contributes to the cycle of how $\delta^{18}O_{SeO4}$ values form and transform in nature. While $\delta^{18}O_{SeO4}$ values in recently formed selenate should be influenced by $\delta^{18}O$ of host water and of oxidants under oxidizing conditions (exposed to atmosphere or light), $\delta^{18}O_{SeO4}$ values can also be enriched during selenate reduction by biogeochemical processes (Schellenger and Larese-Casanova, 2013; Schellenger et al., 2015). The oxygen isotopic information derived from our studies could be combined with selenium isotopic fractionation values (Johnson et al., 1999; Herbel et al., 2000; Johnson et al., 2000; Herbel et al., 2002; Johnson and Bullen, 2003; Ellis et al., 2003; Clark and Johnson, 2010; Schilling et al., 2011b; Schilling et al., 2011a; Schilling et al., 2013; Mitchell et al., 2013; Schilling et al., 2015; Basu et al., 2016; Xu et al., 2020) for interpreting selenium fate and transport

in natural settings.

The kinetic experiments do provide some information on likely kinetic models that could describe these reactions and on which ROS are even possible to oxidize selenite in water. However, our modelling does not include terms for the oxidant concentration, unlike a recent report of selenite oxidation with several other oxidants (Liu et al., 2019). Steady state hydroxyl radical concentrations in surface waters are in the range of 10^{-15} to 10^{-19} M (Minero et al., 2007; Page et al., 2014; Timko et al., 2014), whereas ours was not directly measured during photoproduction but was likely several orders of magnitude higher due to the 200 mM hydrogen peroxide or nitrate provided. Hydrogen peroxide concentrations in surface and rainwaters have been reported in the 10^{-8} to 10^{-5} M range (Cooper et al., 1988; Cooper and Lean, 1989), whereas our experiments included 0.2–2 M. Accordingly, the rates of selenite oxidation to selenate in natural waters by hydroxyl radicals are likely much slower than the rates reported here. With dissolved selenium concentrations in surface waters closer to 10^{-9} to 10^{-5} M, a high relative amount of selenium to ROS might require up to years for any significant selenite conversion to selenate during daylight hours.

Selenite and selenate in surface waters might instead be sourced from environments with greater abundance of oxidants. For one, the highly oxidizing conditions of the atmosphere needs to be evaluated as a place for oxyanion formation during atmospheric transport of selenium species. Several industrial and natural sources contribute to atmospheric selenium emissions annually (Cutter and Cutter, 2001; Mosher and Duce, 1987). Rates are needed for oxidative, atmospheric transformation of elemental selenium and inorganic selenides, similar to organic selenides (Rael et al., 1996). Because atmospheric sulfite oxidation by ozone and hydrogen peroxide is considered important (Ermakov et al., 1997), corresponding reactions for atmospheric selenite might be an order of magnitude slower. Subsequent wet deposition of Se to terrestrial and aquatic environments (Låg and Steinnes, 1974) might transport selenium as oxyanions.

4. Conclusions

Reactive oxygen species were evaluated for selenite oxidation to selenate within batch reactors at circumneutral pH. Of the ROS tested, $^{\bullet}$OH and H_2O_2 could oxidize selenite, but no conclusive evidence for superoxide, singlet oxygen, or peroxynitrite to oxidize selenite was found. The photochemical generation of OH and subsequent oxidation of selenite was much faster for H_2O_2 compared to nitrate or nitrite on an equimolar basis. Selenite oxidation occurring in surface waters, if any, may be part of natural photochemically-driven ROS production and scavenging reactions. Rapid selenite oxidation was also observed with O_3, and this process may be relevant in selenium redox cycling where ozone occurs, i.e. in waters or water vapor in close contact with elevated gaseous ozone concentrations.

Oxidation of selenite by $^{\bullet}$OH, H_2O_2, O_3, and HOCl/OCl$^-$ appears to transfer one O from the oxidant to form selenate. This implies formed selenate in surface waters will have site-specific and process-specific $\delta^{18}O$ values that are controlled by the $\delta^{18}O$ values of host water and the oxidant. This information can be useful in tracing the source, transport, and fate of selenate in natural waters.

Declaration of Competing Interest

The authors declare that they have no known competing financial interests or personal relationships that could have appeared to influence the work reported in this paper.

Acknowledgements

Appendix A. Supplementary data

Supplementary data to this article can be found online at https://doi.org/10.1016/j.chemgeo.2021.120229.

References

Albrecht, S., Zimmermann, T., Grutzmann, R., Scheller, D., Saeger, H., Distler, W., 1999. The redoxsensitive behaviour of selenite in presence of reactive oxygen species. Med. Klin. 94, 70–73.

Andrade, L.H., Pedrozo, E.C., Leite, H.G., Brondani, P.B., 2011. Oxidation of organoselenium compounds. A study of chemoselectivity of phenylacetone monooxygenase. J. Mol. Catal. B 73, 63–66.

Bailey, S., Rapson, T.D., Johnson-Winters, K., Astashkin, A.V., Enemark, J.H., Kappler, U., 2008. Molecular basis for enzymatic sulfite oxidation - how three conserved active site residues shape enzyme activity. J. Biol. Chem. 284, 2053–2063l.

Basu, A., Schilling, K., Brown, S.T., Johnson, T.M., Christensen, J.N., Hartmann, M., Reimus, P.W., Heikoop, J.M., Woldegabriel, G., DePaolo, D.J., 2016. Se isotopes as groundwater redox indicators: Detecting natural attenuation of Se at an in situ recovery U mine. Environ. Sci. Technol. 50, 10833–10842.

Boegel, J.V., Clifford, D.A., 1986. Selenium oxidation and removal by ion exchange. In: United States Environmental Protection Agency EPA/600/S2-86/031, pp. 1–8.

Clark, S.K., Johnson, T.M., 2010. Selenium stable isotope investigation into selenium biogeochemical cycling in a lacustrine environment: Sweitzer Lake, Colorado. J. Environ. Qual. 39, 2200–2210.

Cooper, W.J., Lean, D.R.S., 1989. Hydrogen peroxide concentration in a northern lake: photochemical formation and diel variability. Environ. Sci. Technol. 23, 1425–1428.

Cooper, W.J., Zika, R.G., Petasne, R.G., Plane, J.M.C., 1988. Photochemical formation of hydrogen peroxide in natural waters exposed to sunlight. Environ. Sci. Technol. 22, 1156–1160.

Corsaro, G., 1964. Colorimetric chemical kinetics experiment. J. Chem. Educ. 41, 48.

Cory, R.M., Cotner, J.B., McNeill, K., 2009. Quantifying interactions between singlet oxygen and aquatic fulvic acids. Environ. Sci. Technol. 43, 718–723.

Crawford, J., Hughes, C.E., Parkes, S.D., 2013. Is the isotopic composition of event based precipitation driven by moisture source or synoptic scale weather in the Sydney Basin, Australia? J. Hydrol. 507, 213–226.

Cutter, G.A., Cutter, L.S., 2001. Sources and cycling of selenium in the western and equatorial Atlantic Ocean. Deep-Sea Res. 48, 2917–2931.

Dikshitulu, L.S.A., Babu, R.R., 2009. Kinetic and mechanistic patterns of oxidation of selenium(IV). Prog. React. Kinet. Mech. 34, 97–126.

DiSpirito, A.A., Hooper, A.B., 1986. Oxygen exchange between nitrate molecules during nitrite oxidation by Nitrobacter. J. Biol. Chem. 261, 10534–10537.

Dowdle, P.R., Oremland, R.S., 1998. Microbial oxidation of elemental selenium in soil slurries and bacterial cultures. Environ. Sci. Technol. 32, 3749–3755.

Ellis, A.S., Johnson, T.M., Herbel, M.J., Bullen, T.D., 2003. Stable isotope fractionation of selenium by natural microbial consortia. Chem. Geol. 195, 119–129.

Ermakov, A.N., Poskrebyshev, G.A., Purmal, A.P., 1997. Sulfite oxidation: State-of-the-art of the problem. Kinet. Catal. 38, 295–308.

Fogelman, K.D., Walker, D.M., Margerum, D.W., 1989. Nonmetal redox kinetics: hypochlorite and hypochlorous acid reactions with sulfite. Inorg. Chem. 28, 986–993.

Gao, X., Zhang, J., Zhang, L., 2002. Hollow sphere selenium nanoparticles: their in-vitro anti hydroxyl radical effect. Adv. Mater. 14, 290–293.

Garg, S., Rose, A.L., Waite, T.D., 2011. Photochemical production of superoxide and hydrogen peroxide from natural organic matter. Geochim. Cosmochim. Acta 75, 4310–4320.

Gat, J., 2010. Isotope Hydrology: A Study of the Water Cycle. Imperial College Press, London.

Goff, J., Terry, L., Mal, J., Schilling, K., Pallud, C., Yee, N., 2019. Role of extracellular reactive sulfur metabolites on microbial Se(0) dissolution. Geobiology 17, 320–329.

Gruebel, K.A., Davis, J.A., Leckie, J.O., 1995. Kinetics of oxidation of selenite to selenate in the presence of oxygen, titania, and light. Environ. Sci. Technol. 29, 586–594.

Haag, W.R., Hoigne, J., Gassman, E., Braun, A., 1984. Singlet oxygen in surface waters — part I: Furfuryl alcohol as a trapping agent. Chemosphere 13, 631–640.

Hall, N.F., Alexander, O.R., 1940. Oxygen exchange between anions and water. J. Am. Chem. Soc. 62, 3455–3462.

Henderson, A.K., Shuman, B.N., 2009. Hydrogen and oxygen isotopic compositions of lake water in the western United States. GSA Bull. 121, 1179–1189.

Herbel, M.J., Johnson, T.M., Oremland, R.S., Bullen, T.D., 2000. Fractionation of selenium isotopes during bacterial respiratory reduction of selenium oxyanions. Geochim. Cosmochim. Acta 64, 3701–3709.

Herbel, M.J., Johnson, T.M., Tanji, K.K., Gao, S., Bullen, T.D., 2002. Selenium stable isotope ratios in agricultural drainage water systems of the western San Joaquin Valley, CA. Environ. Qual. 31, 1146–1156.

Hoigné, J., Faust, B.C., Haag, W.R., Scully, F.E., Zepp, R.G., 1988. Aquatic humic substances as sources and sinks of photochemically produced transient reactants. In: Aquatic Humic Substances. American Chemical Society, pp. 363–381.

Howard III, J.H., 1977. Geochemistry of selenium: formation of ferroselite and selenium behavior in the vicinity of oxidizing sulfide and uranium deposits. Geochim. Cosmochim. Acta 41, 1665–1678.

Hughes, F.J., Martin, D.S., 1955. Kinetics of the oxidation of selenious acid by hydrogen peroxide. J. Phys. Chem. 59, 410–415.

Jankowski, J.J., Kieber, D.J., Mopper, K., 1999. Nitrate and nitrite ultraviolet actinometers. Photochem. Photobiol. 70, 319–328.

Johnson, T.M., Bullen, T.D., 2003. Selenium isotope fractionation during reduction by Fe (II)-Fe(III) hydroxide-sulfate (green rust). Geochim. Cosmochim. Acta 67, 413–419.

Johnson, T.M., Herbel, M.J., Bullen, T.D., Zawislanski, P.T., 1999. Selenium isotope ratios as indicators of selenium sources and oxyanion reduction. Geochim. Cosmochim. Acta 63, 2775–2783.

Johnson, T.M., Bullen, T.D., Zawislanski, P.T., 2000. Selenium stable isotope ratios as indicators of sources and cycling of selenium: results from the Northern Reach of San Francisco Bay. Environ. Sci. Technol. 34, 2075–2079.

Jouzel, J., Delaygue, G., Landais, A., Masson-Delmotte, V., Risi, C., Vimeux, F., 2013. Water isotopes as tools to document oceanic sources of precipitation. Water Resour. Res. 49, 7469–7486.

Kaneko, M., Poulson, S.R., 2012. Rate of oxygen isotope exchange between selenate and water. Environ. Sci. Technol. 46, 4539–4545.

Kim, D., Lee, J., Ryu, J., Kim, K., Choi, W., 2014. Arsenite oxidation initiated by the UV photolyiss of nitrite and nitrate. Environ. Sci. Technol. 48, 4030–4037.

Klein, G.W., Bhatia, K., Madhavan, V., Schuler, R.H., 1975. Reaction of hydroxyl radicals with benzoic acid. Isomer distribution in the radical intermediates. J. Phys. Chem. 79, 1767–1774.

Kulp, T.R., Pratt, L.M., 2004. Speciation and weathering of selenium in upper cretaceous chalk and shale from South Dakota and Wyoming, USA. Geochim. Cosmochim. Acta 68, 3687–3701.

Låg, J., Steinnes, E., 1974. Soil selenium in relation to precipitation. Ambio 3, 237–238.

Lakin, H.W., 1961. Geochemistry of selenium in relation to agriculture. In: Anderson, M. S., Lakin, H.W., Beeson, K.C., Smith, F.F., Thacker, E. (Eds.), Selenium in Agriculture, 200. U.S. Dept. of Agric. Handbook, pp. 3–12.

Larese-Casanova, P., Blake, R.E., 2013. Measurement of $\delta^{18}O$ values in arsenic and selenium oxyanions. Rapid Commun. Mass Spectrom. 27, 117–126.

Lawson, S., Macy, J.M., 1995. Bioremediation of selenite in oil refinery wastewater. Appl. Microbiol. Biotechnol. 43, 762–765.

Lemly, A.D., 2004. Aquatic selenium pollution is a global environmental safety issue. Ecotoxicol. Environ. Saf. 59, 44–56.

Li, P., De Marco, A., Feng, Z., Anav, A., Zhou, D., Paoletti, E., 2018. Nationwide ground-level ozone measurements in China suggest serious risks to forests. Environ. Pollut. 237, 803–813.

Liu, Q., Schurter, L.M., Muller, C.E., Aloisio, S., Francisco, J.S., Margerum, D.W., 2001. Kinetics and mechanisms of aqueous ozone reactions with bromide, sulfite, hydrogen sulfite, iodide, and nitrite Ions. Inorg. Chem. 40, 4436–4442.

Liu, S., Salhi, E., Huang, W., Diao, K., von Gunten, U., 2019. Kinetic and mechanistic aspects of selenite oxidation by chlorine, bromine, monochloramine, ozone, permanganate, and hydrogen peroxide. Water Res. 164, 114876.

Lu, K., Zhu, J.-M., Xu, W.-P., Tan, D.-C., 2017. The kinetic study on the abiotic oxidation of elemental selenium I: oxidation by hydrogen peroxide. Bull. Mineral. Petrol. Geochem. 36, 75–81.

Lunenok-Burmakina, V.H., Kusakovskaya, T.M., Miroshnichenko, A.G., 1967. Use of Oxygen Isotopes for Studying the Oxidation of Inorganic Ions by Hydrogen Peroxide and Ozone, 3, p. 146.

Luoma, S.N., Presser, T.S., 2009. Emerging opportunities in management of selenium contamination. Environ. Sci. Technol. 43, 8483–8487.

Martens, D.A., Suarez, D.L., 1997. Selenium speciation of marine shales, alluvial soils, and evaporation basin soils of California. J. Environ. Qual. 26, 424–432.

Masscheleyn, P.H., Delaune, R.D., Patrick, W.H., 1990. Transformations of selenium as affected by sediment oxidation-reduction potential and pH. Environ. Sci. Technol. 24, 91–96.

Minero, C., Chiron, S., Falletti, G., Maurino, V., Pelizzetti, E., Ajassa, R., Carlotti, M.E., Vione, D., 2007. Photocheminal processes involving nitrite in surface water samples. Aquat. Sci. 69, 71–85.

Mitchell, K., Couture, R., Johnson, T.M., Mason, P.R.D., Van Cappellen, P., 2013. Selenium sorption and isotope fractionation: iron(III) oxides versus iron(II) sulfides. Chem. Geol. 342, 21–28.

Mosher, B.W., Duce, R.A., 1987. A global atmospheric selenium budget. J. Geophys. Res. 92, 13289–13298.

Mostofa, K.M.G., Liu, C., Sakugawa, H., Vione, D., Minakata, D., Saquib, M., Mottaleb, M. A., 2013. Photoinduced generation of hydroxyl radical in natural waters. In: Mostofa, K.M.G., Yoshioka, T., Mottaleb, A., Vione, D. (Eds.), Photobiogeochemistry of Organic Matter: Principles and Practices in Water Environments. Springer Berlin Heidelberg, Berlin, Heidelberg, pp. 209–272.

Okumura, A., Okazaki, N., 1973a. Kinetics of oxygen exchange between selenate ions and water. Bull. Chem. Soc. Jap. 46, 1080–1084.

Okumura, A., Okazaki, N., 1973b. Kinetics of oxygen exchange between selenite ions and water. Bull. Chem. Soc. Jap. 46, 1084–1088.

Page, S.E., Logan, J.R., Cory, R.M., McNeill, K., 2014. Evidence for dissolved organic matter as the primary source and sink of photochemically produced hydroxyl radical in arctic surface waters. Environ Sci Process Impacts 16, 807–822.

Presser, T.S., 1994. The Kestersen effect. Environ. Manag. 18, 437–454.

Presser, T.S., Swain, W.C., 1990. Geochemical evidence for Se mobilization by the weathering of pyritic shale, San Joaquin Valley, California, U.S.A. Appl. Geochem. 5, 703–717.

Rael, R.M., Tuzaon, E.C., Frankenberger, W.T., 1996. Gas-phase reactions of dimethyl selenide with ozone and the hydroxyl and nitrate radicals. Atmos. Environ. 30, 1221–1232.

Rice, E.W., Baird, R.B., Eaton, A.D., Clesceri, L.S., 2012. Standard Methods for the Examination of Water and Wastewater. American Public Health Association, American Water Works Association, Water Environment Federation.

Ripperton, L.A., Jeffries, H., Worth, J.J.B., 1971. Natural synthesis of ozone in the troposphere. Environ. Sci. Technol. 5, 246–248.

Sánchez-Polo, M., von Gunten, U., Rivera-Utrilla, J., 2005. Efficiency of activated carbon to transform ozone into OH radicals: Influence of operational parameters. Water Res. 39, 3189–3198.

Sarathchandra, S.U., Watkinson, J.H., 1981. Oxidation of elemental selenium to selenite by *Bacillus megaterium*. Science 211, 600–601.

Schellenger, A.E.P., Larese-Casanova, P., 2013. Oxygen isotope indicators of selenate reaction with Fe(II) and Fe(III) hydroxides. Environ. Sci. Technol. 47, 6254–6262.

Schellenger, A.E.P., Onnis-Hayden, A., Jaisi, D.P., Larese-Casanova, P., 2015. Oxygen kinetic isotope effects in selenate during microbial reduction. Appl. Geochem. 63, 261–271.

Schellenger, A.E.P., Choi, S., Onnis-Hayden, A., Larese-Casanova, P., 2021. Selenium oxyanion exchange with Mg(II)-Fe(III) and Fe(II)-Fe(III) layered double hydroxides. Appl. Clay Sci. 200, 105959.

Schilling, K., Johnson, T.M., Wilcke, W., 2011a. Isotope fractionation of selenium during fungal biomethylation by *Alternaria alternata*. Environ. Sci. Technol. 45, 2670–2676.

Schilling, K., Johnson, T.M., Wilcke, W., 2011b. Selenium partitioning and stable isotope ratios in urban topsoils. Soil Sci. Soc. Am. J. 75, 1354–1364.

Schilling, K., Johnson, T.M., Wilcke, W., 2013. Isotope fractionation of selenium by biomethylation in microcosm incubations of soil. Chem. Geol. 352, 101–107.

Schilling, K., Johnson, T.M., Dhillon, K.S., Mason, P.R.D., 2015. Fate of selenium in soils at a seleniferous site recorded by high precision Se isotope measurements. Environ. Sci. Technol. 49, 9690–9698.

Scott, M.J., Morgan, J.J., 1996. Reactions at oxide surfaces. 2. Oxidation of Se(IV) by synthetic birnessite. Environ. Sci. Technol. 30, 1990–1996.

Seiler, R.L., Skorupa, J.P., Peltz, L.A., 1999. Areas susceptible to irrigation-induced selenium contamination of water and biota in the western United States. USGS Circular 1180, 1–36.

Sillman, S., 1999. The relation between ozone, NOx and hydrocarbons in urban and polluted rural environments. Atmos. Environ. 33, 1821–1845.

Sotelo, J.L., Beltran, F.J., Benitez, F.J., Beltran-Heredia, J., 1987. Ozone decomposition in water: kinetic study. Ind. Eng. Chem. Res. 26, 39–43.

Stillings, L.L., Amacher, M.C., 2010. Kinetics of selenium release in mine waste from the Meade Peak Phosphatic Shale, Phosphoria Formation, Wooley Valley, Idaho, USA. Chem. Geol. 269, 113–123.

Strawn, D., Doner, H., Zavarin, M., McHugo, S., 2002. Microscale investigation into the geochemistry of arsenic, selenium, and iron in soil developed in pyritic shale materials. Geoderma 108, 237–257.

Timko, S.A., Romera-Castillo, C., Jaffé, R., Cooper, W.J., 2014. Photo-reactivity of natural dissolved organic matter from fresh to marine waters in the Florida Everglades, USA. Environ Sci Process Impacts 16, 866–878.

US EPA, 1987. Estimated National Occurrence and Exposure to Nitrate and Nitrite in Public Drinking Water Supplies, United States Environmental Protection Agency. Office of Drinking Water, Washington, DC.

Vaughan, P.P., Blough, N.V., 1998. Photochemical formation of hydroxyl radical by constituents of natural waters. Environ. Sci. Technol. 32, 2947–2953.

Vijayaraghavan, K., Cho, S., Morris, R., Spink, D., Jung, J., Pauls, R., Duffett, K., 2016. Photochemical model evaluation of the ground-level ozone impacts on ambient air quality and vegetation health in the Alberta oil sands region: using present and future emission scenarios. Atmos. Environ. 141, 209–218.

Winterrath, T., Kurosu, T.P., Richter, A., Burrows, J.P., 1999. Enhanced O_3 and NO_2 in thunderstorm clouds: Convection or production? Geophys. Res. Lett. 26, 1291–1294.

Xia, L., Schellenger, A.E.P., Onnis-Hayden, A., Jaisi, D., Larese-Casanova, P., 2020. Isolation of selenate from selenite, carbonate, phosphate, and arsenate solutions for δ^{18}O-selenate determination. Isot. Environ. Health Stud. 1–17. https://doi.org/10.1080/10256016.2020.1733552.

Xu, W., Zhu, J., Johnson, T.M., Wang, X., Lin, Z., Tan, D., Qin, H., 2020. Selenium isotope fractionation during adsorption by Fe, Mn and Al oxides. Geochim. Cosmochim. Acta 272, 121–136.

Zafiriou, O.C., True, M.B., 1979. Ntirate photolysis in seawater by sunlight. Mar. Chem. 8, 33–42.

Zellner, R., Exner, M., Herrmann, H., 1990. Absolute OH quantum yields in the laser photolysis of nitrate, nitrite and dissolved H_2O_2 at 308 and 351 nm in the temperature range 278-353K. J. Atmos. Chem. 10, 411–425.

Zepp, R.G., Wolfe, N.L., Baughman, G.L., Hollis, R.C., 1977. Singlet oxygen in natural waters. Nature 267, 421–423.

Zhang, J., Tang, H., Zhu, J., Lin, X., Feng, Y., 2019. Effects of elevated ground-level ozone on paddy soil bacterial community and assembly mechanisms across four years. Sci. Total Environ. 654, 505–513.